

1 ***Plxna1* and *Plxna3* cooperate to pattern the nasal axons that guide gonadotropin-**
2 **releasing hormone neurons**

3

4 Roberto Oleari¹, Alessia Caramello^{2,3}, Sara Campinoti^{2,3}, Antonella Lettieri¹, Elena
5 Ioannou², Alyssa Paganoni¹, Alessandro Fantin^{2,4}, Anna Cariboni^{1,2*}, Christiana
6 Ruhrberg^{2*}.

7

8 ¹ University of Milan, Department of Pharmacological and Biomolecular Sciences, Via G.
9 Balzaretti 9, 20133 Milan, Italy

10 ² UCL Institute of Ophthalmology, University College London, 11-43 Bath Street, London
11 EC1V 9EL, UK

12 ³ current address: The Francis Crick Institute, 1 Midland Road, London NW1 1AT, UK

13 ⁴ current address: University of Milan, Department of Biosciences, Via G. Celoria 26,
14 20133, Milan, Italy

15 * to whom correspondence should be addressed:

16 anna.cariboni@unimi.it or c.ruhrberg@ucl.ac.uk

17

18

19 **Keywords:** GnRH neuron, olfactory bulb, testes, axon guidance, plexin, semaphorin,
20 hypogonadotropic hypogonadism, Kallmann Syndrome

21

22 **Running title:** PLXNAs in GnRH neuron migration

23

24 **Summary statement:** PLXNA1 and PLXNA3 convey the pathfinding of olfactory and
25 vomeronasal axons as a prerequisite for neuroendocrine neurons to migrate into the
26 hypothalamus and release gonadotropins into the circulation.

27 **Abstract**

28

29 The gonadotropin releasing hormone (GnRH) neurons regulate puberty onset and sexual
30 reproduction by secreting GnRH to activate and maintain the hypothalamic-pituitary-
31 gonadal axis. During embryonic development, GnRH neurons migrate along olfactory and
32 vomeronasal axons through the nose into the brain, where they project to the median
33 eminence to release GnRH. The secreted glycoprotein SEMA3A binds its receptors
34 neuropilin (NRP) 1 or NRP2 to position these axons for correct GnRH neuron migration,
35 with an additional role for the NRP co-receptor PLXNA1. Accordingly, mutations
36 in *SEMA3A*, *NRP1*, *NRP2* and *PLXNA1* have been linked to defective GnRH neuron
37 development in mice and inherited GnRH deficiency in humans. Here, we show that only
38 the combined loss of *PLXNA1* and *PLXNA3* phenocopied the full spectrum of nasal axon
39 and GnRH neuron defects of *SEMA3A* knockout mice. Together with *Plxna1*, the human
40 ortholog of *Plxna3* should therefore be investigated as a candidate gene for inherited
41 GnRH deficiency.

42

43 **Introduction:**

44 GnRH-secreting neurons are hypothalamic neuroendocrine cells that regulate sexual
45 reproduction in mammals by stimulating the pituitary secretion of the gonadotropins
46 luteinizing hormone (LH) and follicle-stimulating hormone (FSH) (Merchenthaler et al.,
47 1984). GnRH deficiency is the common hallmark of two genetic reproductive disorders,
48 hypogonadotropic hypogonadism (HH) and Kallmann syndrome (KS), which can be due to
49 defective GnRH neuron development (Boehm et al., 2015; Stamou and Georgopoulos,
50 2018).

51 A key period in GnRH neuron development is their migration from the nasal placode,
52 where they are born, to their final positions in the hypothalamus. In the nasal
53 compartment, GnRH neurons migrate along the intermingled axons of olfactory (OLF) and
54 vomeronasal (VN) neurons, whose cell bodies are located in the nasal placode-derived
55 olfactory epithelium (OE) and vomeronasal organ (VNO), respectively (**Fig. S1A**). To enter
56 the brain, GnRH neurons migrate along the caudal branch of the VN (cVN) nerve, also
57 known as the cranial nerve 0 or terminal nerve (Taroc et al., 2017; Yoshida et al., 1995).
58 The axons in this transient nerve turn caudo-ventrally into the brain at the level of the
59 cribriform plate (CP), which separates the brain from the nasal compartment (Taroc et al.,
60 2017) (**Fig. S1A**). Instead, other VN and OLF axons project to the main and the accessory
61 olfactory bulb (OB), respectively (**Fig. S1A**). Finally, GnRH neurons settle in the medial
62 preoptic area (MPOA) of the postnatal hypothalamus to project to the median eminence
63 (ME), where they act as neuroendocrine cells to release GnRH into the hypophyseal portal
64 circulation (Wierman et al., 2011) (**Fig. S1B**). Accordingly, GnRH neurons can be identified
65 in several distinct compartments of the embryonic head that reflect their migratory route
66 (**Fig. S1C**).

67 The importance of proper axon scaffolds for GnRH neuron migration is illustrated by the
68 analysis of a human foetus with a KS mutation; in this foetus, GnRH neurons accumulated
69 in neural tangles in the meninges at the level of CP (Schwanzel-Fukuda et al., 1989). Mice
70 lacking the axon guidance cue SEMA3A similarly accumulate GnRH neurons within axon
71 tangles at the CP and are therefore hypogonadal (Cariboni et al., 2011). Moreover, they
72 have defective olfactory system, with many aberrant OLF axons (Schwartz et al., 2004).
73 Agreeing with combined GnRH neurons and olfactory defects in mice lacking SEMA3A,
74 *SEMA3A* mutations were subsequently identified in a subset of KS patients (Hanchate et
75 al., 2012; Young et al., 2012). These findings support the idea that proper axon guidance
76 is essential to ensure GnRH neuron migration through the nose and into the brain.

77 Moreover, these findings illustrate that mouse models are powerful tools to uncover genes
78 that regulate GnRH neuron development and may be mutated in patients with inherited
79 GnRH neuron deficiency.

80 To exert its functions, SEMA3A usually binds to transmembrane receptors composed of a
81 ligand binding subunit that is either neuropilin (NRP) 1 or NRP2, and a signal transducing
82 subunit, typically a member of the A-type plexin (PLXNA) family (Alto and Terman, 2017).
83 Accordingly, mice lacking SEMA3A signalling through NRP1 and NRP2 have similar axon
84 and GnRH neuron defects as mice lacking SEMA3A (Cariboni et al., 2011). Mutations in
85 *NRP1*, *NRP2* and *PLXNA1* have also been found in KS patients (Kotan et al., 2019;
86 Marcos et al., 2017), although *PLXNA1* loss affects the GnRH neuron and olfactory
87 systems in mice only mildly (Marcos et al., 2017). These findings raise the possibility that
88 *PLXNA1* acts in partial redundancy with another A-type plexin. Here, we have compared
89 the expression pattern of all four *Plxna* genes during GnRH neuron development in the
90 mouse and examined whether *Plxna1* synergises with *Plxna3* during nasal axon guidance
91 required for proper GnRH neuron migration.

92

93 **Results and discussion:**

94

95 ***Plxna1* and *Plxna3* are co-expressed during GnRH neuron migration.**

96 To establish which of the four *Plxna* genes is expressed in a pattern consistent with a role
97 in guiding the axons that ensure GnRH neuron migration, we performed *in situ*
98 hybridisation of sections through the wild type mouse embryo nose. Agreeing with prior
99 reports (Marcos et al., 2017; Murakami et al., 2001; Suto et al., 2003), *Plxna1* was
100 expressed at E12.5 and E14.5 in both the VNO and OE, and *Plxna3* had a similar
101 expression pattern (**Fig. S2A,B**). Additionally, *Plxna1* and *Plxna3* transcripts were
102 detected in the migratory mass (MM) (**Fig. S2A**), a mixed population of cells that includes
103 neurons and olfactory ensheathing cells (OECs) (Miller et al., 2010). In contrast, *Plxna2*
104 and *Plxna4* appeared only weakly expressed in the VNO, OE or MM cells (**Fig. S2A**). We
105 therefore focussed subsequent work on *Plxna1* and *Plxna3*.

106 To determine which cell types expressed PLXNA1 or PLXNA3 in the territories relevant to
107 GnRH neuron migration, we immunostained sections through wild type mouse embryo
108 heads. Double labelling with the TUJ1 antibody for neuronal-specific beta 3 tubulin
109 (nTUBB3) showed that PLXNA1 and PLXNA3 localised to the MM at E12.5 and to axons
110 emerging from the OE and VNO at E12.5 and E14.5 (**Fig. 1A,B**). Double labelling for the

111 OEC marker S100 showed that OECs lacked PLXNA1 and PLXNA3, but that they
112 surrounded PLXNA1/PLXNA3 double-positive axons (**Fig. 1C,D**). Immunostaining of
113 *Plxna1*^{-/-} and *Plxna3*^{-/-} mouse tissues validated antibody specificity (**Fig. 1E**). Double
114 labelling for peripherin (PRPH), a marker of OLF and VN, including cVN axons (Fueshko
115 and Wray, 1994; Taroc et al., 2017), confirmed that both PLXNs localised to E14.5 nasal
116 axons; PLXNA1 was also prominent on cVN axons in the forebrain, whereas PLXNA3
117 staining of cVN axons was undetectable (**Fig. 2**). A prior study reported PLXNA1
118 immunostaining of E12.5 GnRH neurons (Marcos et al., 2017); in agreement, we observed
119 low *Plxna1* transcript levels in FACS-isolated E13.5 GnRH neurons (Cariboni et al., 2007).
120 Nevertheless, GnRH neurons in the E14.5 nose and ventral forebrain lacked obvious
121 PLXNA1 or PLXNA3 (**Fig. 2**).

122 Together, these findings raise the possibility that PLXNA1 and PLXNA3 pattern the axons
123 that guide GnRH neurons, either directly or by regulating the behaviour of pioneer cells in
124 the MM that act as guide-post cells for the first nasal axons (Miller et al., 2010).
125 Additionally, GnRH neurons may themselves express PLXNA1 for some time during their
126 development.

127 ***Reduced GnRH neuron migration into the forebrain of Plxna1/Plxna3-null embryos***

128 We next investigated whether combined loss of PLXNA1 and PLXNA3 impairs GnRH
129 neuron migration more severely than loss of PLXNA1 alone. Thus, we analysed the
130 number and position of GnRH neurons in wild type, single and double mutant embryos in
131 litters from parents carrying *Plxna1*-null and *Plxna3*-null alleles (Cheng et al., 2001;
132 Yoshida et al., 2006). GnRH immunostaining showed that *Plxna1*^{-/-} and *Plxna3*^{-/-} single as
133 well as *Plxna1*^{-/-};*Plxna3*^{-/-} double mutants had an overall similar number of GnRH neurons
134 compared to wild type littermates at E14.5 (**Fig. 3A,C** and **Table S1**). Whereas *Plxna1*^{-/-}
135 and *Plxna3*^{-/-} single mutants had a similar number of neurons as wild types in the forebrain,
136 *Plxna1*^{-/-};*Plxna3*^{-/-} double mutants contained significantly fewer GnRH neurons in the
137 forebrain (**Fig. 3A,C** and **Table S1**). The loss of GnRH neurons from the brain of *Plxna1*^{-/-}
138 ;*Plxna3*^{-/-} double mutants was explained by the statistically significant retention of GnRH
139 neurons in the nose, including at the CP (**Fig. 3B,C** and **Table S1**). Similar results were
140 obtained by *Gnrh* *in situ* hybridisation (**Fig. S3A**). As the overall number of GnRH neurons
141 was similar in all these genotypes at this stage, the primary GnRH neuron defect in double
142 mutants is likely the impaired forebrain entry.

143 ***Combined PLXNA1 and PLXNA3 loss increases morbidity and causes GnRH***

144 **neuron, gonadal and olfactory system defects**

145 To assess whether lack of GnRH neurons in the forebrain of E14.5 *Plxna1*^{-/-};*Plxna3*^{-/-}
146 embryos results in an hypogonadal state in adulthood, we analysed postnatal *Plxna1*^{-/-}
147 ;*Plxna3*^{-/-} mice. The analysis of 5 litters from parents with combined *Plxna1*-null and
148 *Plxna3*-null alleles suggested that all genotypes were born at a normal Mendelian ratio
149 (**Table S2**), but there was a high rate of pre-weaning mortality. As the *Plxna3* gene resides
150 on the X chromosome, males in these litters are either wild type or hemizygous for the
151 *Plxna3*-null mutation, i.e. *Plxna3*^{+/+} or *Plxna3*^{Y/-}, respectively. In contrast, females are
152 *Plxna3*^{+/+}, *Plxna3*^{+/-} or *Plxna3*^{-/-}. Pooled male and female mice lacking *Plxna3* are therefore
153 referred to as *Plxna3*^{-/(y)}. We found that 2/5 juvenile *Plxna1*^{-/-};*Plxna3*^{-/(y)} mutants were
154 small and appeared stressed when handled and had to be culled before weaning to
155 prevent suffering. To avoid the birth of further mutants with such severe adverse effects,
156 breeding was concluded, and all mutants obtained culled for analyses.

157 We next compared the GnRH neuron number in the MPOA of postnatal mutants and wild
158 type controls, because this is the final position these neurons should attain. Whereas the
159 GnRH neuron number in the *Plxna3*^{Y/-} MPOA was similar to that of wild type littermates,
160 3/5 *Plxna1*^{-/-} mutants had slightly fewer and 4/4 *Plxna1*^{-/-};*Plxna3*^{-/(y)} mutants contained
161 hardly any GnRH neurons in the MPOA (**Fig. 3D,E** and **Table S3**). Agreeing with a
162 severely reduced GnRH neuron number, GnRH staining of the ME was nearly absent in
163 *Plxna1*^{-/-};*Plxna3*^{-/(y)} mutants (**Fig. 3F**), despite normal hypothalamic projections of
164 neuroendocrine neurons, such as those that secrete the corticotropin releasing hormone
165 CRH (**Fig. S3B**). Moreover, overall brain size was similar in all genotypes (**Table S4**). All
166 genotypes also had similar OB sizes (**Table S4**), but *Plxna1*^{-/-};*Plxna3*^{-/(y)} mutants had a
167 smaller glomerular layer (GL) in the dorso-lateral OB compared to single mutants or wild
168 types (**Fig. S4**). Accordingly, the combined loss of PLXNA1 and PLXNA3 causes defects
169 in both the GnRH neuron and olfactory systems, the two co-existing hallmarks of KS.

170 Consistent with hypothalamic GnRH deficiency, 3/3 *Plxna1*^{-/-};*Plxna3*^{-/(y)} mutants had
171 smaller gonads compared to single mutant littermates and wild types (2/2 males lacking
172 both PLXNA1 and PLXNA3 had smaller testes and seminiferous vesicles, and 1/1 female
173 lacking both PLXNA1 and PLXNA3 had smaller ovaries; **Fig. 3G-H**; **Fig. S5A,B**). Notably,
174 1/2 *Plxna1*^{-/-};*Plxna3*^{Y/-} males examined only had one testis (**Fig. S5A**) and double mutant
175 testes appeared immature and contained hardly any spermatids (**Fig. S5C**). We also
176 detected PLXNA1 (Perälä et al., 2005) and PLXNA3 expression in the seminiferous
177 tubules and interstitial cells of the testes, but not in the ovary or pituitary (**Fig. S5D-F**).

178 Thus the severe testes phenotype of double mutants may result from the combined tissue-
179 specific loss of both plexins and hypothalamic GnRH deficiency.

180 A prior study reporting KS-like symptoms in adult *Plxna1*^{-/-} mice had focussed on the
181 analysis of males (Fig. 3 in Marcos et al., 2017). As we observed a genetic interaction of
182 *Plxna1* and *Plxna3*, it is conceivable that the mild and only partially penetrant defect
183 observed in *Plxna1*^{-/-} males might be explained, at least in part, by the hemizygous state of
184 *Plxna3* in males that impacts on GnRH neuron development. However, it is not known
185 whether *Plxna3* hemizyosity contributes to the increased incidence of KS in males
186 compared to females. Notably, 2/2 adult *Plxna1*^{-/-};*Pxna3*^{+/-} females had a severe reduction
187 of GnRH neurons in the MPOA, which exceeded that seen in 3/5 *Plxna1*^{-/-} male mutants
188 (**Table S3**). The intermediate phenotype severity in these females between *Plxna1*^{-/-} single
189 and *Plxna1*^{-/-};*Pxna3*^{+/-} double mutants may be explained by random X chromosome
190 inactivation, as this has the potential to remove the functional copy of PLXNA3 in *Pxna3*^{+/-}
191 females and thereby decrease PLXNA3 dosage. Further work would be required to
192 investigate this hypothesis.

193

194 ***Mispatterned OLF/VN axons in *Plxna1/Plxna3*-null embryos form axon tangles at the*** 195 ***cribriform place that retain GnRH neurons***

196 To better understand the underlying cause of abnormal GnRH neuron migration during
197 embryogenesis, we examined the patterning of their PRPH⁺ axonal migratory scaffolds in
198 E14.5 embryos from parents carrying both *Plxna1*⁻ and *Plxna3*-null alleles. This was also
199 important, because nasal axon defects were previously reported in 5/18 E14.5 *Plxna1*^{-/-}
200 mutants (Marcos et al., 2017). We found that 3/3 *Plxna1*^{-/-} and 3/3 *Plxna3*^{-/-} single mutants
201 had similar PRPH⁺ axon organisation as wild type littermates, whereas 3/3 *Plxna1*^{-/-}
202 ;*Plxna3*^{-/-} double mutants contained PRPH⁺ mistargeted axons between the OBs and axon
203 tangles at the CP (**Fig. 4A,B**). These axon defects therefore occur in areas in which GnRH
204 neurons accumulate (**Fig. 4B**; see also **Fig. 3B**). Even though cVN axons emerged from
205 the VNO in all genotypes analysed (**Fig. S6A**), double mutants lacked cVN axons in the
206 forebrain (**Fig. 4A,B**). Moreover, double, but not single null mutants, had defasciculated
207 and enlarged OLF axon bundles below the ventro-medial OBs (**Fig. S6B**) that may explain
208 the small size of the glomerular layer (GL) in the OB of double null mutants (see **Fig. S4**).

209 In summary, the combined loss of PLXNA1 and PLXNA3 severely disrupts the axons that
210 guide GnRH neurons through the nose and into the brain and additionally impairs olfactory
211 development. Notably, the axonal defects are similar to those reported for *Sema3a*-null

212 mutants (Cariboni et al., 2011; Hanchate et al., 2012), supporting the idea that PLXNA1
213 and PLXNA3 serve as co-receptors for SEMA3A during VN and OLF axon development.
214 Interestingly, partial PLXNA redundancy for SEMA3A-mediated axon targeting mirrors the
215 redundancy for SEMA3A's ligand binding receptors, as loss of semaphorin signalling
216 through both NRP1 and NRP2 is required to elicit the full spectrum of VN and OLF as well
217 as GnRH neuron migration defects that is observed in *Sema3a*-null mutants (Cariboni et
218 al., 2007; Cariboni et al., 2011).

219

220 **Conclusion.** Here we show that PLXNA1 and PLXNA3 cooperate to pattern the
221 SEMA3A/NRP-dependent axons that serve as migratory scaffolds for GnRH neurons *en*
222 *route* from the nasal placodes to the brain and also contribute to olfactory axon patterning.
223 Accordingly, the loss of both PLXNA1 and PLXNA3 from nasal axons impairs the
224 development of the GnRH neuron and olfactory systems to cause a KS-like phenotype in
225 adult mice (see working model, **Fig. 4C**). The human ortholog of *Plxna3*, like *PLXNA1*,
226 should thus be considered a candidate gene for mutation screening in patients with KS.
227 We further observed severe defects in testes formation in PLXNA1 and PLXNA3 mice that
228 exceed those seen in KS, suggesting that these genes might also be mutated in other
229 congenital diseases that affect gonad formation.

230

231 **Acknowledgements:** We thank Yutaka Yoshida, Alex Kolodkin and Valerie Castellani for
232 the knockout mice, Laura Denti, Vasiliki Chantzara, Jessica Gimmelli and James Brash for
233 technical assistance, John Parnavelas for access to equipment, the Biological Resources
234 Unit of the UCL Institute of Ophthalmology for mouse husbandry and the imaging facilities
235 at UCL and the Università degli Studi di Milano for maintaining microscopes.

236

237 **Methods:**

238 **Mouse strains.** Mice lacking *Plxna1* or *Plxna3* (Cheng et al., 2001; Yoshida et al., 2006)
239 were used in a C57/Bl6 background for all embryonic studies or on a CD1 background to
240 increase postnatal survival of double mutants. As the *Plxna3* gene resides on the X
241 chromosome, we have indicated whether postnatal mice were male (*Plxna3*^{Y/-}) or female
242 (*Plxna3*^{X/-}) and have referred to groups of both sexes as *Plxna3*^{-/- (Y)}; the sex of mouse
243 embryos was not determined, and we therefore refer to all embryos lacking PLXNA3 as
244 *Plxna3*^{-/-}. To obtain mouse embryos of defined gestational ages, mice were mated in the
245 evening, and the morning of vaginal plug formation was counted as embryonic day (E) 0.5.

246 Due to the severe phenotype in 5/5 postnatal double mutants in the 5 litters obtained, we
247 abandoned further crosses to obtain additional adult mutants due to ethical considerations.
248 Genotyping protocols can be supplied on request. All animal procedures were performed
249 in accordance with Animal Welfare Ethical Review Body (AWERB) guidelines and under
250 UK Home Office licence and Italian Ministry of Health licences.

251 **Tissue preparation and cryosectioning:** E12.5 and E14.5 embryos were fixed for 3
252 hours in 4% formaldehyde, whereas post-natal tissues were dissected after perfusion in
253 4% formaldehyde. All samples were then cryoprotected overnight in 30% sucrose,
254 included in OCT and cryosectioned for immunohistochemistry or *in situ* hybridisation.
255 Schematic drawings showing the anatomical levels and orientation of the sections are
256 displayed in **Fig. S7**.

257 ***In situ* hybridisation.** Formaldehyde-fixed cryosections were incubated with digoxigenin
258 (DIG)-labelled anti-sense riboprobes for mouse *Plxna1*, *Plxna2*, *Plxna3* or *Plxna4*
259 (Addgene plasmids no. 58237, 62353, 58238 and 58239, respectively; Schwarz et al.,
260 2008) or mouse *Gnrh* (Cariboni et al., 2015). For labelling, we used the DIG RNA labelling
261 kit (Roche). Hybridisation was performed in 50% formamide, 0.3 M sodium chloride, 20
262 mM Tris pH 7.5, 5 mM EDTA, 10% dextran sulphate and 1x Denhardt's solution overnight
263 at 65°C. Sections were washed in a saline sodium citrate buffer (50% formamide, 1x
264 saline sodium citrate buffer, 0.1% Tween20), incubated overnight with alkaline
265 phosphatase (AP)-conjugated anti-DIG IgG (1:1500; Roche) and developed overnight at
266 37°C with 4-nitro blue tetrazolium chloride and 5-bromo-4-chloro-3-indolyl phosphate
267 disodium salt (Roche) dissolved in a buffer comprised of 100 mM Tris pH 9.5, 50 mM
268 MgCl₂, 100 mM NaCl and 1% Tween 20.

269 **Immunofluorescence labelling.** 25 µm cryostat sections of formaldehyde-fixed embryos
270 were incubated with serum-free protein block (DAKO) after permeabilisation of sections
271 with 0.1% TritonX-100. We used as primary antibodies rabbit anti-peripherin (1:100;
272 Merck Millipore, cat. no. AB1530), rabbit anti-GnRH, previously validated to recognise both
273 the pre-hormone and the processed hormone (Taroc et al., 2019) (1:400; Immunostar, cat.
274 no. 20075), rabbit anti-S100 (1:400, DAKO, cat. no. Z0311), mouse anti-TUBB3 (1:500,
275 clone Tuj1, Covance, cat. no. MMS- 435P), goat anti-OMP (1:200 WAKO, cat. no. 019-
276 22291), goat anti-PLXNA1 (1:200; R&D Systems, cat. no. AF4309) and goat anti-PLXNA3
277 (1:200; R&D Systems, cat. no. AF4075). Secondary antibodies used were Cy3-conjugated
278 donkey anti-goat and 488-conjugated donkey anti-rabbit Fab fragments (1:200; Jackson
279 Immunoresearch). Nuclei were counterstained with DAPI (1:10000; Sigma).

280 **Immunoperoxidase labelling.** 25 μm cryostat sections of formaldehyde-fixed samples
281 were incubated with hydrogen peroxide to quench endogenous peroxidase activity, and
282 sequentially incubated with 10% heat-inactivated normal goat serum in PBS or serum-free
283 blocking solution (DAKO) and then immunostained with the above antibodies to GnRH
284 (1:1000), PLXNA1 (1:500) and PLXNA3 (1:500) or antibodies to CRH (1:400, Proteintech,
285 cat. no. 10944-1-AP) and an appropriate species-specific biotinylated antibody (1:400;
286 Vector Laboratories). Sections were developed with the ABC kit (Vector Laboratories) and
287 3,3-diaminobenzidine (DAB; Sigma). To determine the total number of GnRH neurons at
288 E14.5, 25 μm coronal sections through each entire head were immunolabelled for GnRH
289 and all GnRH-positive cells in the nose, CP area and forebrain were counted, as
290 previously reported (Cariboni et al., 2011; Cariboni et al., 2015). To help distinguish
291 individual GnRH neurons found in cell clumps at the CP of double mutants, high
292 magnification images were analysed. To determine the number of GnRH neurons in the
293 MPOA of postnatal adult male brains, 25 μm coronal sections through the MPOA from a
294 position around 200 μm after the end of ME to the area in which the two hemispheres
295 separate (60 sections/brain) were immunolabelled and all GnRH-positive cells counted in
296 all sections.

297 **Haematoxylin and eosin staining (H&E).** 8 μm sections of formaldehyde-fixed testes
298 from P60 mice were stained as previously described (Macchi et al., 2017).

299 **Statistical analysis.** Sample sizes for expression and mouse phenotyping analyses were
300 estimated based on prior experience and those in the existent literature. Typically, embryo
301 samples were taken from at least three different litters for each group. Randomization was
302 not used to assign samples to experimental groups or to process data, but samples were
303 allocated to groups based on genotypes. The researcher analysing the data was blind to
304 the genotypes during analysis. Loss of sections during cryosectioning of embryo heads,
305 damaged tissue and unspecific immunostaining were pre-established criteria for sample
306 exclusion, otherwise all samples were included in the analyses. All data are expressed as
307 mean \pm standard deviation (s.d.); error bars represent the standard deviation. We used a
308 one-way ANOVA followed by a Dunnett's test to determine the statistical significance
309 between values in multiple comparisons; a *P*-value of <0.05 was considered significant; *P*-
310 values of <0.05 , <0.01 , <0.001 or <0.0001 were indicated with one, two, three or four
311 asterisks, respectively. Statistical analysis was performed using Prism4 software
312 (GraphPad Software, San Diego, CA, USA).

313

314 **Competing interests:** The authors have no competing or financial interests to declare.

315 **Author contributions:** R.O. performed experiments, analysed data and contributed to
316 manuscript writing; A. Caramello, S.C., A.L., A.P., A.F. and E.I. performed experiments; A.
317 Cariboni and C.R. designed experiments, analysed and interpreted results and wrote the
318 manuscript.

319 **Funding:** This research was funded by the Biotechnology and Biological Sciences
320 Research Council (BB/L002639/1) to C.R., Fondazione Telethon (GGP13142) and
321 CHARGE Foundation to A. Cariboni. R.O. received a Boehringer Ingelheim Fonds travel
322 fellowship.

323

324 **References:**

325 **Alto, L. T. and Terman, J. R.** (2017). Semaphorins and their Signaling Mechanisms.
326 *Methods Mol. Biol.* **1493**, 1–25.

327 **Boehm, U., Bouloux, P.-M., Dattani, M. T., de Roux, N., Dodé, C., Dunkel, L., Dwyer,**
328 **A. A., Giacobini, P., Hardelin, J.-P., Juul, A., et al.** (2015). Expert consensus
329 document: European Consensus Statement on congenital hypogonadotropic
330 hypogonadism--pathogenesis, diagnosis and treatment. *Nat. Rev. Endocrinol.* **11**,
331 547–64.

332 **Cariboni, A., Hickok, J., Rakic, S., Andrews, W., Maggi, R., Tischkau, S. and**
333 **Parnavelas, J. G.** (2007). Neuropilins and their ligands are important in the migration
334 of gonadotropin-releasing hormone neurons. *J. Neurosci.* **27**, 2387–95.

335 **Cariboni, A., Davidson, K., Rakic, S., Maggi, R., Parnavelas, J. G. and Ruhrberg, C.**
336 (2011). Defective gonadotropin-releasing hormone neuron migration in mice lacking
337 SEMA3A signalling through NRP1 and NRP2: implications for the aetiology of
338 hypogonadotropic hypogonadism. *Hum. Mol. Genet.* **20**, 336–44.

339 **Cariboni, A., André, V., Chauvet, S., Cassatella, D., Davidson, K., Caramello, A.,**
340 **Fantin, A., Bouloux, P., Mann, F. and Ruhrberg, C.** (2015). Dysfunctional SEMA3E
341 signaling underlies gonadotropin-releasing hormone neuron deficiency in Kallmann
342 syndrome. *J. Clin. Invest.* **125**, 2413–28.

343 **Cheng, H. J., Bagri, A., Yaron, A., Stein, E., Pleasure, S. J. and Tessier-Lavigne, M.**
344 (2001). Plexin-A3 mediates semaphorin signaling and regulates the development of
345 hippocampal axonal projections. *Neuron* **32**, 249–263.

346 **Fueshko, S. and Wray, S.** (1994). LHRH cells migrate on peripherin fibers in embryonic
347 olfactory explant cultures: an in vitro model for neurophilic neuronal migration. *Dev.*
348 *Biol.* **166**, 331–48.

349 **Hanchate, N. K., Giacobini, P., Lhuillier, P., Parkash, J., Espy, C., Fouveaut, C.,**
350 **Leroy, C., Baron, S., Campagne, C., Vanacker, C., et al.** (2012). SEMA3A, a gene
351 involved in axonal pathfinding, is mutated in patients with Kallmann syndrome. *PLoS*
352 *Genet.* **8**, e1002896.

353 **Kotan, L. D., Isik, E., Turan, I., Mengen, E., Akkus, G., Tastan, M., Gurbuz, F., Yuksel,**
354 **B. and Topaloglu, A. K.** (2019). Prevalence and associated phenotypes of PLXNA1
355 variants in normosmic and anosmic idiopathic hypogonadotropic hypogonadism. *Clin.*
356 *Genet.* **95**, 320–324.

357 **Macchi, C., Steffani, L., Oleari, R., Lettieri, A., Valenti, L., Dongiovanni, P., Romero-**
358 **Ruiz, A., Tena-Sempere, M., Cariboni, A., Magni, P., et al.** (2017). Iron overload
359 induces hypogonadism in male mice via extrahypothalamic mechanisms. *Mol. Cell.*
360 *Endocrinol.* **454**, 135–145.

361 **Marcos, S., Monnier, C., Rovira, X., Fouveaut, C., Pitteloud, N., Ango, F., Dodé, C.**
362 **and Hardelin, J.-P.** (2017). Defective signaling through plexin-A1 compromises the
363 development of the peripheral olfactory system and neuroendocrine reproductive axis
364 in mice. *Hum. Mol. Genet.* **26**, 2006–2017.

365 **Merchenthaler, I., Görcs, T., Sétáló, G., Petrusz, P. and Flerkó, B.** (1984).
366 Gonadotropin-releasing hormone (GnRH) neurons and pathways in the rat brain. *Cell*
367 *Tissue Res.* **237**, 15–29.

368 **Miller, A. M., Treloar, H. B. and Greer, C. A.** (2010). Composition of the migratory mass
369 during development of the olfactory nerve. *J. Comp. Neurol.* **518**, 4825–41.

370 **Murakami, Y., Suto, F., Shimizu, M., Shinoda, T., Kameyama, T. and Fujisawa, H.**
371 (2001). Differential expression of plexin-A subfamily members in the mouse nervous
372 system. *Dev. Dyn.* **220**, 246–58.

373 **Perälä, N. M., Immonen, T. and Sariola, H.** (2005). The expression of plexins during
374 mouse embryogenesis. *Gene Expr. Patterns* **5**, 355–62.

375 **Schwanzel-Fukuda, M., Bick, D. and Pfaff, D. W.** (1989). Luteinizing hormone-releasing
376 hormone (LHRH)-expressing cells do not migrate normally in an inherited
377 hypogonadal (Kallmann) syndrome. *Mol. Brain Res.*

378 **Schwarz, Q., Waimey, K. E., Golding, M., Takamatsu, H., Kumanogoh, A., Fujisawa,**
379 **H., Cheng, H. and Ruhrberg, C.** (2008). Plexin A3 and plexin A4 convey semaphorin
380 signals during facial nerve development. *Dev. Biol.* **324**, 1–9.

381 **Stamou, M. I. and Georgopoulos, N. A.** (2018). Kallmann syndrome: phenotype and
382 genotype of hypogonadotropic hypogonadism. *Metabolism.* **86**, 124–134.

383 **Suto, F., Murakami, Y., Nakamura, F., Goshima, Y. and Fujisawa, H.** (2003).
384 Identification and characterization of a novel mouse plexin, plexin-A4. *Mech. Dev.*
385 **120**, 385–96.

386 **Taroc, E. Z. M., Prasad, A., Lin, J. M. and Forni, P. E.** (2017). The terminal nerve plays a
387 prominent role in GnRH-1 neuronal migration independent from proper olfactory and
388 vomeronasal connections to the olfactory bulbs. *Biol. Open* **6**, 1552–1568.

389 **Taroc, E. Z. M., Lin, J. M., Tulloch, A. J., Jaworski, A. and Forni, P. E.** (2019). GnRH-1
390 Neural Migration From the Nose to the Brain Is Independent From Slit2, Robo3 and
391 NELL2 Signaling. *Front. Cell. Neurosci.* **13**, 70.

392 **Wierman, M. E., Kiseljak-Vassiliades, K. and Tobet, S.** (2011). Gonadotropin-releasing
393 hormone (GnRH) neuron migration: initiation, maintenance and cessation as critical
394 steps to ensure normal reproductive function. *Front. Neuroendocrinol.* **32**, 43–52.

395 **Yoshida, K., Tobet, S. a, Crandall, J. E., Jimenez, T. P. and Schwarting, G. a** (1995).
396 The migration of luteinizing hormone-releasing hormone neurons in the developing rat
397 is associated with a transient, caudal projection of the vomeronasal nerve. *J.*
398 *Neurosci.* **15**, 7769–77.

399 **Yoshida, Y., Han, B., Mendelsohn, M. and Jessell, T. M.** (2006). PlexinA1 signaling
400 directs the segregation of proprioceptive sensory axons in the developing spinal cord.
401 *Neuron* **52**, 775–88.

402 **Young, J., Metay, C., Bouligand, J., Tou, B., Francou, B., Maione, L., Tosca, L.,**
403 **Sarfati, J., Brioude, F., Esteva, B., et al.** (2012). SEMA3A deletion in a family with
404 Kallmann syndrome validates the role of semaphorin 3A in human puberty and
405 olfactory system development. *Hum. Reprod.* **27**, 1460–5.

406

407 **Figure legends:**

408

409 **Figure 1. Expression of PLXNA1 and PLXNA3 on neuronal cell bodies and axons.**

410 (A,B) Expression of PLXNA1 and PLXNA3 on neurons and axons. Coronal sections of
411 E12.5 (A) and E14.5 (B) mouse heads were immunolabelled at the level of the VNO for
412 nTUBB3 together with PLXNA1 or PLXNA3. The corresponding single PLXNA1 or
413 PLXNA3 channels are shown below each image. White boxes indicate areas shown at
414 higher magnification on the right of the corresponding panel. Arrows and arrowheads
415 indicate examples of PLXNA1 and PLXNA3-positive neurons and axons, respectively.

416 (C,D) PLXNA1 and PLXNA3 are not expressed by S100-positive cells. Coronal sections of
417 E12.5 (C) and E14.5 (D) mouse heads at VNO level were immunolabelled for S100 to
418 detect OECs and PLXNA1 or PLXNA3. White boxes indicate areas shown at higher
419 magnification on the right of the corresponding panel. Clear arrowheads indicate lack of
420 PLXNA1 or PLXNA3 co-localisation with S100.

421 (E) Specificity of PLXNA1 and PLXNA3 antibodies. Coronal sections from E14.5 *Plxna1*-
422 and *Plxna3*-null mice at VNO level were immunostained for PLXNA1 or PLXNA3; lack of
423 staining indicates antibody specificity.

424 All sections were counterstained with DAPI.

425 Abbreviations: OE, olfactory epithelium; OB, olfactory bulb; NS, nasal septum; VNO,
426 vomeronasal organ; OEC, olfactory ensheathing cells.

427 Scale bars: 150 or 50 μ m for lower and higher magnifications, respectively.

428

429 **Figure 2. PLXNA1 and PLXNA3 localise to nasal axons.**

430 (A-D) Coronal sections of E14.5 mouse heads were immunolabelled for PLXNA1 (A,B) or
431 PLXNA3 (C,D) together with PRPH (top panels) or GnRH (bottom panels). Sections are
432 shown at the level of the VNO (nose) or MPOA (forebrain). White boxes indicate areas
433 shown at higher magnification on the right of the corresponding panel, with single
434 channels shown also adjacent to the panel. Arrowheads in (A-C) indicate examples of
435 PRPH-positive axons with PLXNA1 and PLXNA3, respectively. Clear arrowheads in (D)
436 indicate examples of PRPH-positive axons that lack PLXNA3. Clear arrows in (A-D)
437 indicate examples of GnRH neurons that lack PLXNA1 and PLXNA3, respectively. All
438 sections were counterstained with DAPI.

439 Abbreviations: OE, olfactory epithelium; OB, olfactory bulb; VNO, vomeronasal organ;
440 MPOA, medial preoptic area.

441 Scale bars: 150 or 50 μm for lower and higher magnifications, respectively.

442

443 **Figure 3. Combined PLXNA1 and PLXNA3 loss decreases GnRH neuron number, ME**
444 **innervation and testes size in adult mice.**

445 (A-C) Embryonic GnRH neuron analysis. (A) Coronal sections of E14.5 mouse heads with
446 the indicated genotypes were immunolabelled for GnRH. The OB boundaries are indicated
447 with black dotted lines in the wild type panel. Arrowheads indicate examples of GnRH
448 neurons at the CP (top panels), in the nasal parenchyma (middle panels) and in the MPOA
449 (bottom panels). The black arrow and open arrowheads indicate GnRH neuron clumps
450 between the OBs and at the CP, respectively. Δ indicates a lack of GnRH neurons in the
451 MPOA. (B) High magnification image of double mutant E14.5 embryo showing example of
452 GnRH neurons accumulated cells at the CP and between OBs. (C) Quantification of GnRH
453 neuron number in the E14.5 head; data are shown as mean \pm s.d.; *** $P < 0.001$, ** $P < 0.01$,
454 * $P < 0.05$ (one way ANOVA with Dunnett's test).

455 (D-F) Adult GnRH neuron analysis. Coronal sections of P60 brains with the indicated
456 genotypes at the level of the MPOA (D) and ME (F) were immunolabelled for GnRH. Δ
457 indicates a lack of GnRH staining. (E) Quantification of GnRH neuron number in the P60
458 MPOA; data are shown as mean \pm s.d.; * $P < 0.05$, **** $P < 0.0001$ (one way ANOVA with
459 Dunnett's test).

460 (G-H) Adult gonad size. Micrographs show paired testes (G, left panel), seminal vesicles
461 (G, right panel) and ovaries (H) of P60 littermate mice.

462 Abbreviations: OB, olfactory bulb; CP, cribriform plate; MPOA, medial preoptic area; ME,
463 median eminence; sem. ves., seminal vesicles.

464 Scale bars: 150 μm (A,E), 500 μm (C), 3 mm (F,G), 1.5 mm (H).

465

466 **Figure 4. Combined PLXNA1 and PLXNA3 loss impairs nasal axon and GnRH**
467 **neuron distribution.**

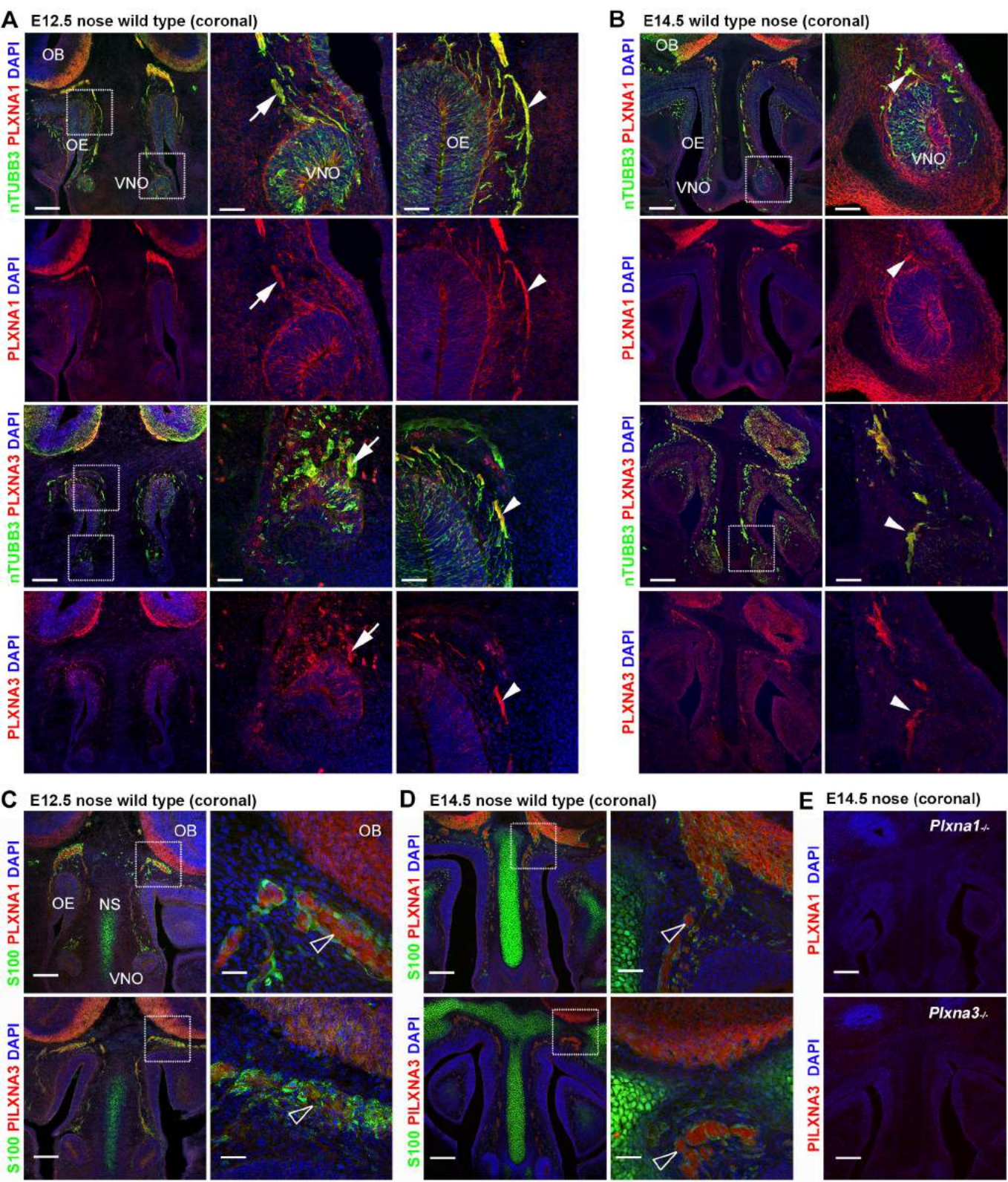
468 (A,B) Adjacent coronal sections of E14.5 mouse heads of the indicated genotypes at the
469 level of the CP (A) and MPOA (B) were immunolabelled for PRPH to reveal OLF, VN and
470 cVN axons (top panels) and GnRH neurons (bottom panels). The OB boundaries are

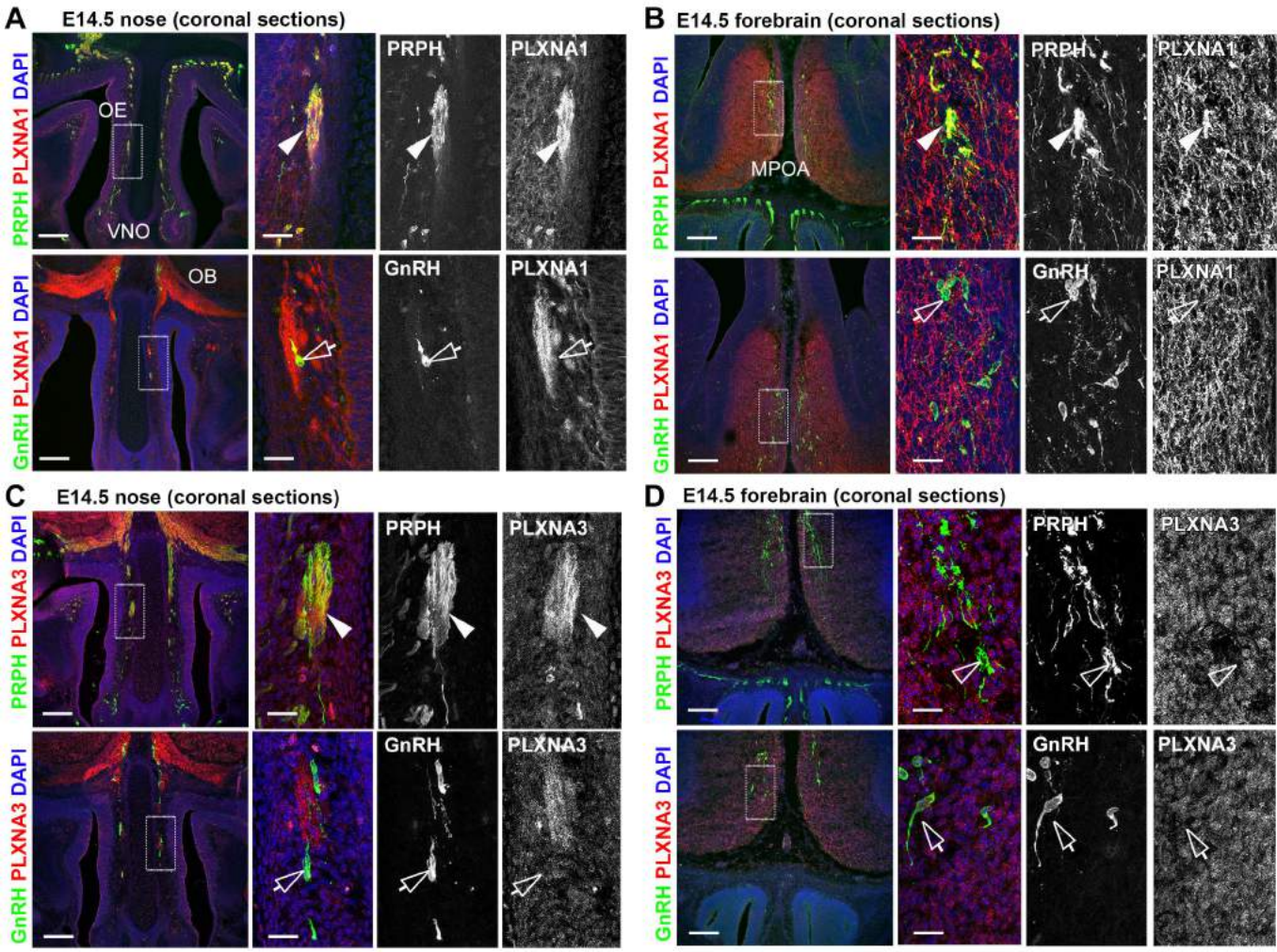
471 indicated with dotted lines in the wild type panel. Solid arrows and open arrowheads
472 indicate examples of ectopic axons and GnRH neurons between the OBs and at the CP,
473 respectively. Solid arrowheads indicate cVN axons in the MPOA. A lack of GnRH neurons
474 and cVN axons in the MPOA is indicated with Δ .

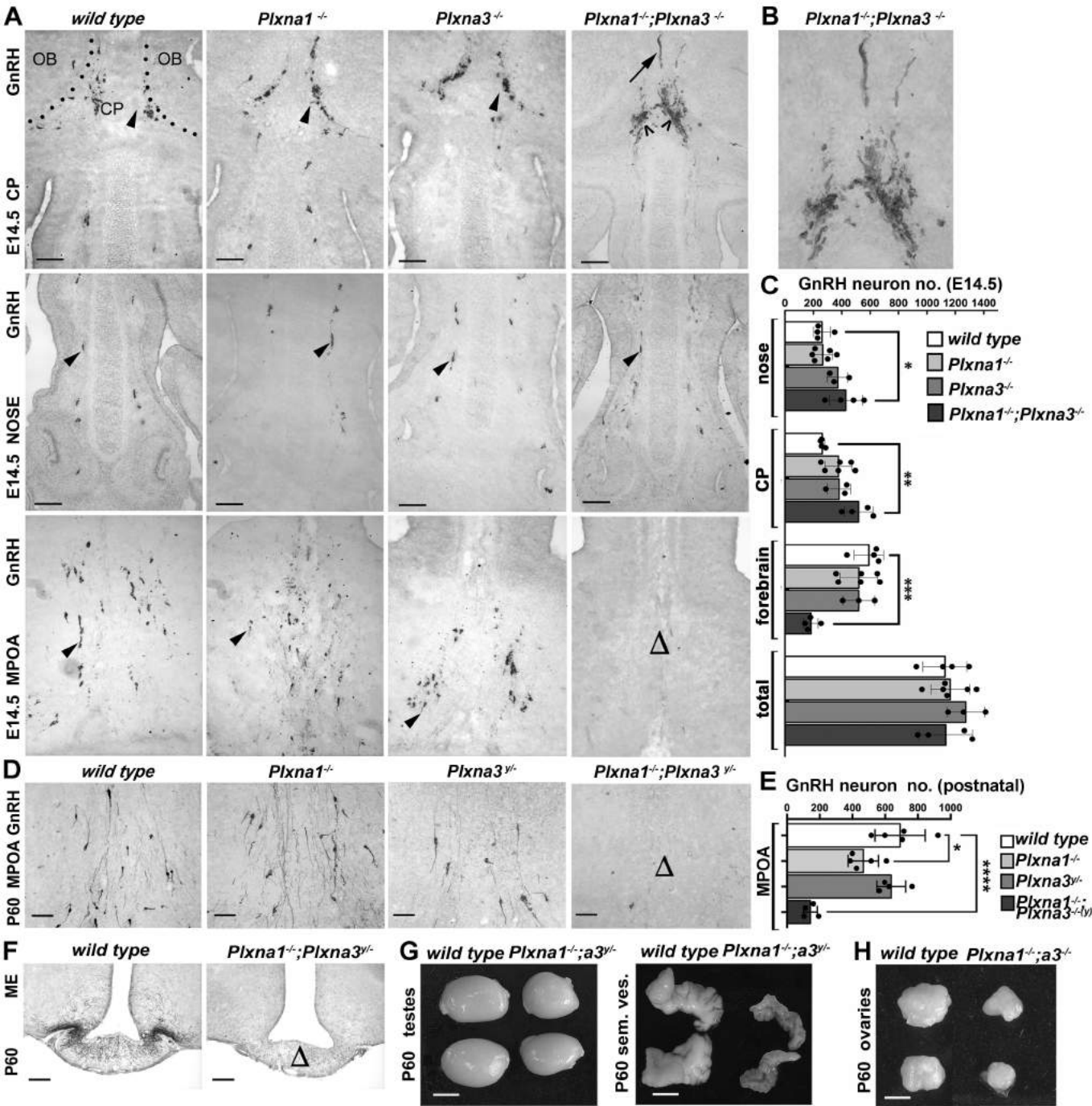
475 Abbreviations: OB, olfactory bulb; CP, cribriform plate; MPOA, medial preoptic area.

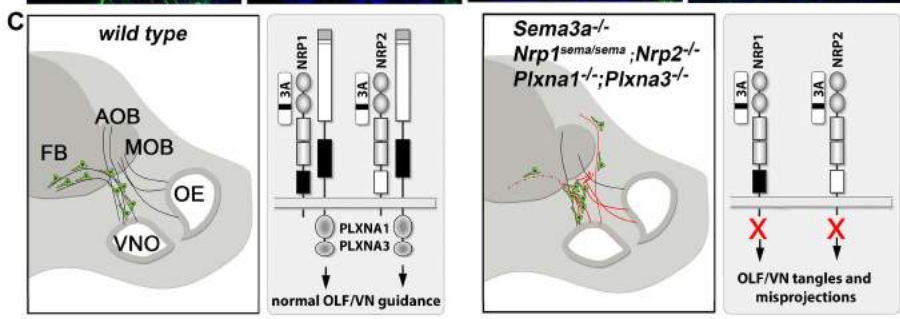
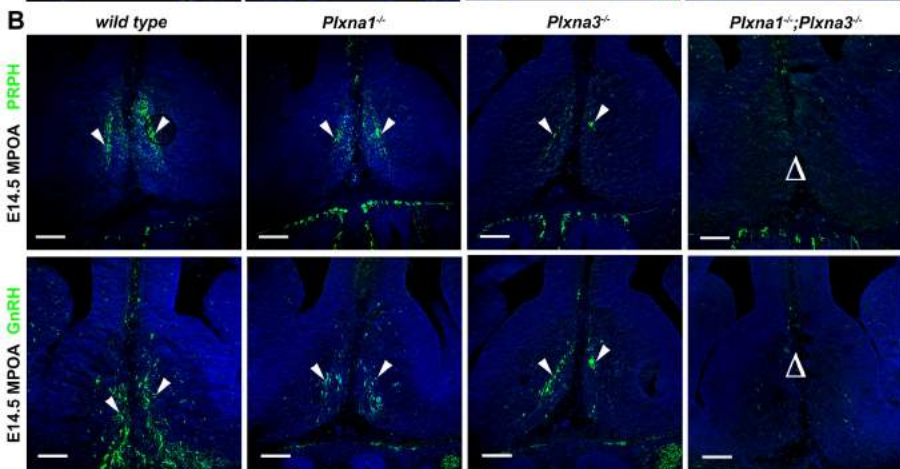
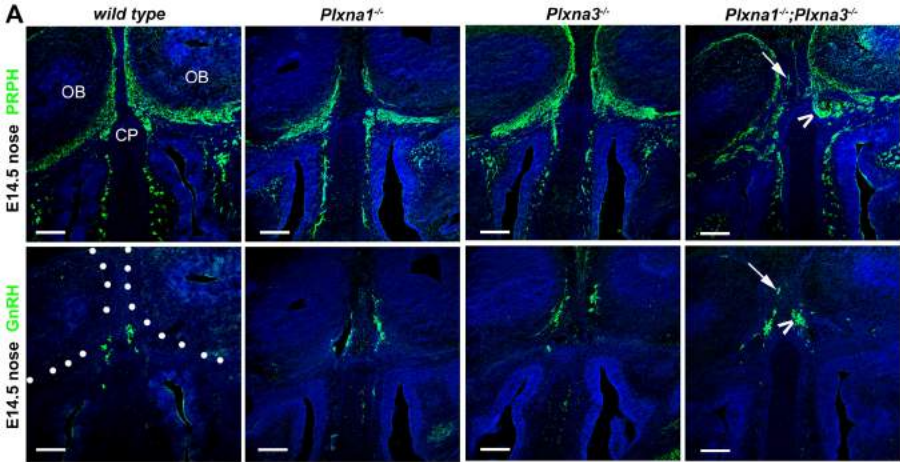
476 Scale bar: 150 μ m.

477 (C) Working model summarising the observed defects in GnRH neuron (green) migration
478 and axon organisation in wild type embryos vs. SEMA3A pathway mutants. Normal axon
479 projections are shown as continuous black lines, abnormal projections are shown as
480 continuous red line; the interrupted red line in mutants represents the missing cVN branch.
481 The corresponding, predicted signalling pathways are shown adjacent to each head
482 schematic.









SUPPLEMENTARY MATERIAL

6 supplementary figures with legends

4 supplementary tables

Fig. S1

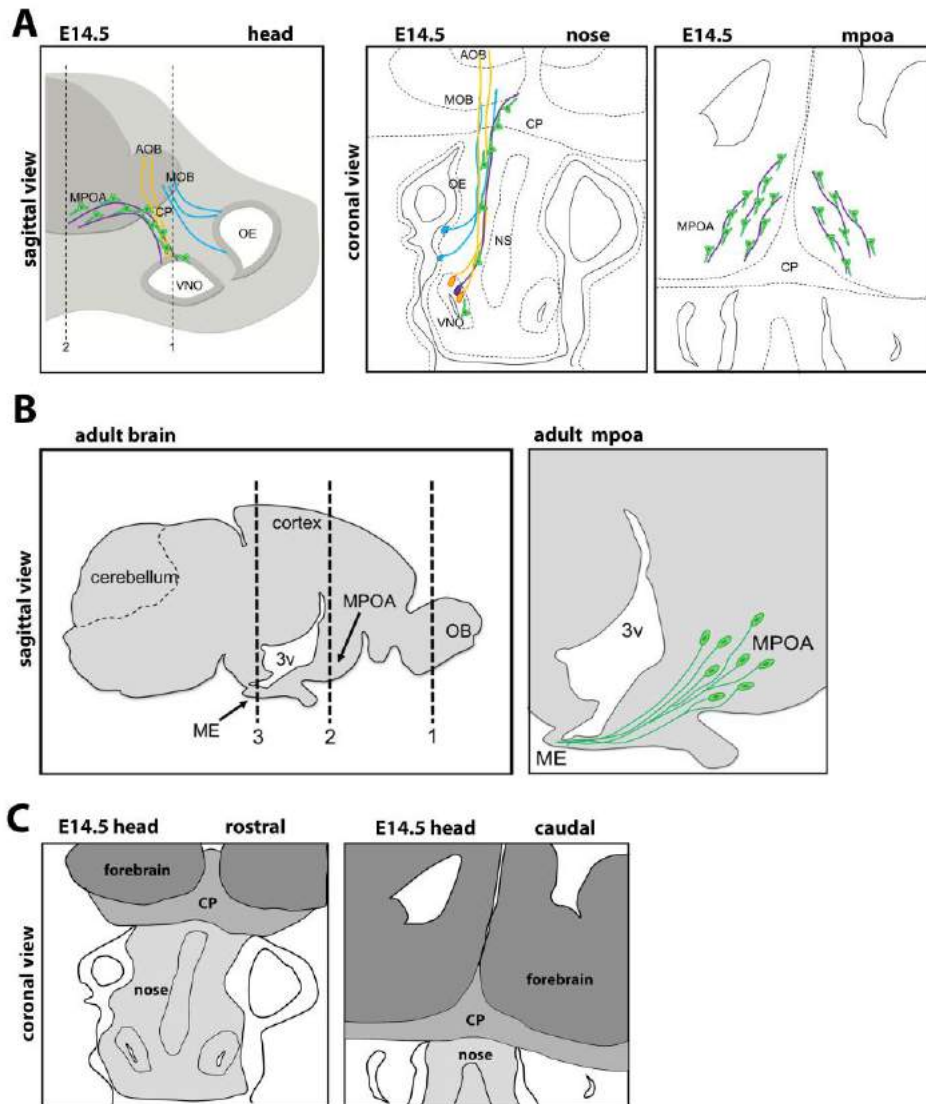


Fig. S1. Head structures relevant to GnRH neuron migration and position.

(A) Sagittal view of an E14.5 mouse head; dashed lines (1, 2) indicate the anatomical levels at which coronal sections were obtained for immunostaining in this study. The adjacent schematics show coronal views of the structures present in these sections. Nasal axons and their cell bodies are differently colored: OLF axons in blue, VN in orange and cVN/TN in purple; GnRH neurons are shown in green.

(B) Sagittal view of an adult brain; dashed lines (1-3) indicate the anatomical levels at which coronal sections were obtained for immunostaining in this study. The adjacent schematic shows that GnRH neurons in the adult MPOA project their axons towards the ME.

(C) Coronal view of an E14.5 mouse head at nasal (left panel) and MPOA (right panel) level. The anatomical compartments referred to in this study and used as reference points for GnRH neuron number quantifications are distinguished by different shades of grey.

Abbreviations: OB, olfactory bulb; MPOA, medial preoptic area; VNO, vomeronasal organ; NS, nasal septum; CP, cribriform plate; ME, median eminence, 3v, third ventricle.

Fig. S2

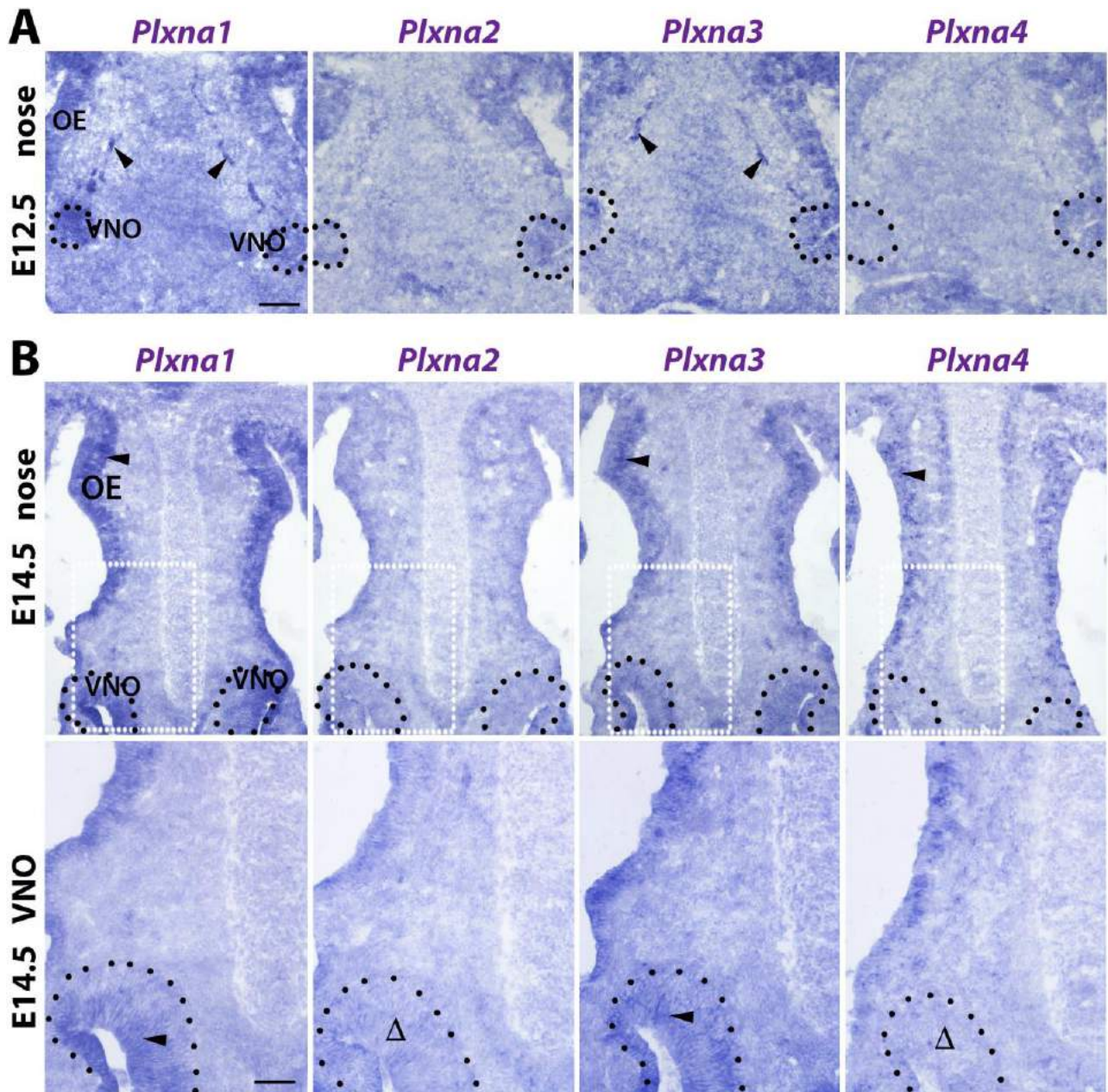


Fig. S1. *Plxna* expression in the mouse embryo nose.

In situ hybridisation to examine the expression of the indicated *Plxna* genes, performed with coronal sections from E12.5 (A) and E14.5 (B) mouse heads at the level of the VNO. Higher magnifications of the boxed areas are shown below each image. The black dots delineate the VNO. Arrowheads in (A) indicate examples of *Plxna1*- or *Plxna3*-positive cells that appear to be migrating from the VNO. Arrowheads in (B) indicate expression of *Plxna1*, *Plxna3* and *Plxna4* in the olfactory epithelium (OE, top row) or expression of *Plxna1* and *Plxna3* in the VNO (bottom row). Δ indicates lack of *Plxna2* and *Plxna4* expression in the VNO in (B).

Scale bars: 150 μ m (A, top row in B), 100 μ m (bottom row in B).

Abbreviations: VNO, vomeronasal organ; OE, olfactory epithelium.

Fig. S3

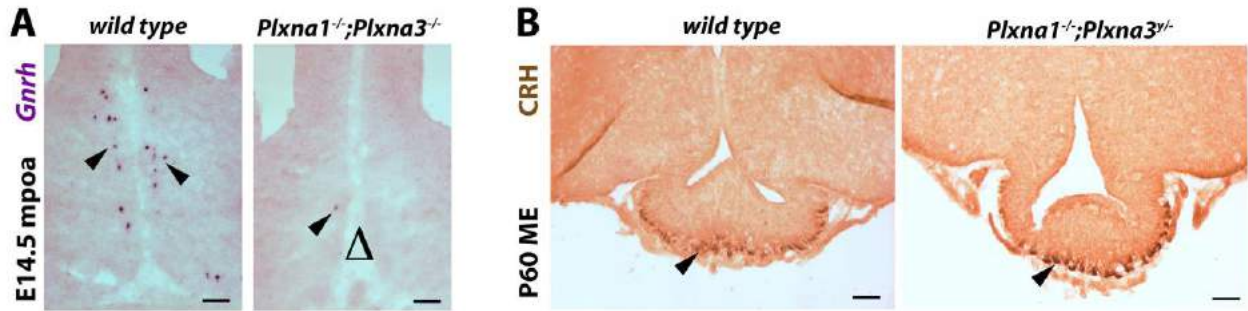


Fig. S3. GnRH deficiency is not due to loss of GnRH peptide synthesis or an absent ME.

(A) *In situ* hybridisation for the *Gnrh* transcript on coronal sections of E14.5 mouse heads at the level of the medial preoptic area (MPOA) in the indicated genotypes. Arrowheads indicate *Gnrh*-expressing neurons. Lack of *Gnrh*⁺ cells in the *Plxna1^{-/-};Plxna3^{-/-}* MPOA is indicated with Δ .

(B) Median eminence (ME) innervation by corticotropin-releasing hormone (CRH)⁺ fibers in coronal sections of a P60 *Plxna1^{-/-};Plxna3^{-/-}* mutant and littermate wildtype control.

Scale bars: 150 μ m.

Fig. S4

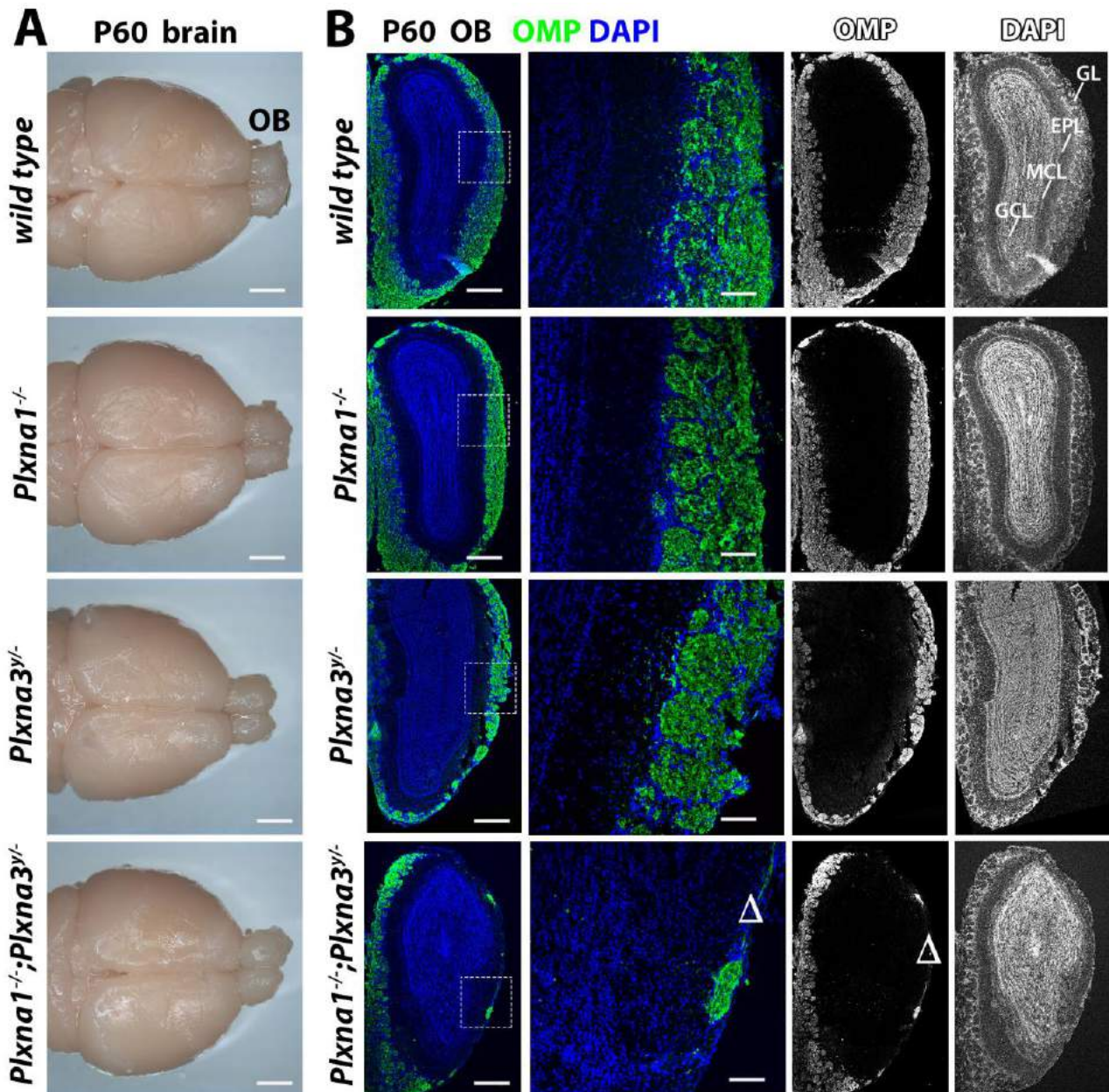


Fig. S4. Impaired OB development in mice lacking PLXNA1 and PLXNA3.

(A) Micrographs of P60 brains from mice of the indicated genotypes. The brain and olfactory bulbs (OBs) appear to be of similar size in all genotypes (see Supplemental Table 4 for quantification).

(B) Coronal sections of P60 OBs from mice of the indicated genotypes were immunolabelled for OMP to reveal OB innervation and counterstained with DAPI. Higher magnifications of the boxed areas are shown adjacent to each image. Δ indicates a near absent glomerular layer (GL) in the dorso-lateral region of double mutants.

Scale bars: 3 mm (A), 500 and 100 μm (lower and higher magnifications in B, respectively).

Abbreviations: OB, olfactory bulb; GL, glomerular layer; EPL, external plexiform layer; MCL mitral cell layer; IPL, inner plexiform layer.

Fig. S5

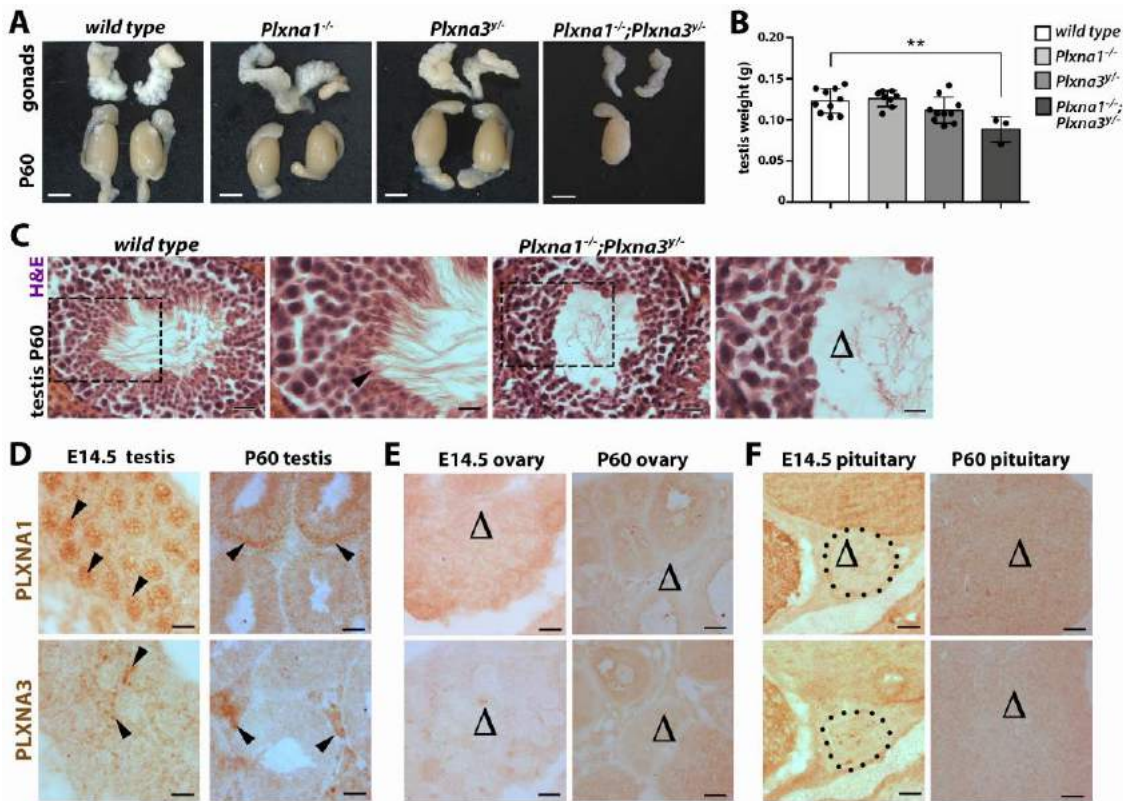


Fig. S5. PLXNA1 and PLXNA3 cooperate for testis formation but are not expressed in the ovaries or pituitary gland.

(A) Micrographs show pairs of seminal vesicles (top) and testes (bottom) in P60 mice of the indicated genotypes. The double mutant shown had only one testis. Scale bar: 3 mm.

(B) Individual testis weights in the indicated genotypes at P60. Data are shown as mean \pm s.d., and P-values compared to wild type were calculated by one-way ANOVA followed by a Dunnett's test; wildtype 0.123 ± 0.015 g (n = 10 testes); *Plxna1*^{-/-} 0.126 ± 0.010 g (n = 8 testes), P > 0.05 (not significant); *Plxna3*^{y/-} 0.112 ± 0.016 g (n = 10 testes), P > 0.05 (not significant); *Plxna1*^{-/-};*Plxna3*^{y/-} 0.0849 ± 0.016 g (n = 3 testes), **P < 0.01.

(C) Haematoxylin and eosin (H & E) staining of P60 testes illustrate seminiferous tubules in wild type and double mutant mice; black boxes indicate areas shown at higher magnification adjacent to each image. The arrowhead indicates spermatozoa within the lumen of seminiferous tubules; Δ indicates near absence of spermatozoa. Scale bars: 50 μ m or 25 μ m for lower and higher magnifications, respectively.

(D-F) Expression analysis for PLXNA1 and PLXNA3. Cryosections of wild type E14.5 and P60 testis (D), ovary (E) and pituitary (circled in F) were immunolabelled for PLXNA1 (upper panels) or PLXNA3 (lower panels). Arrowheads in (D) indicate PLXNA1 localisation to seminiferous tubule cells and PLXNA3 localisation to interstitial cells. Lack of PLXNA1 or PLXNA3 expression in (E,F) is indicated with Δ . Scale bars: 150 μ m (E14.5) and 50 μ m (P60).

Fig. S6

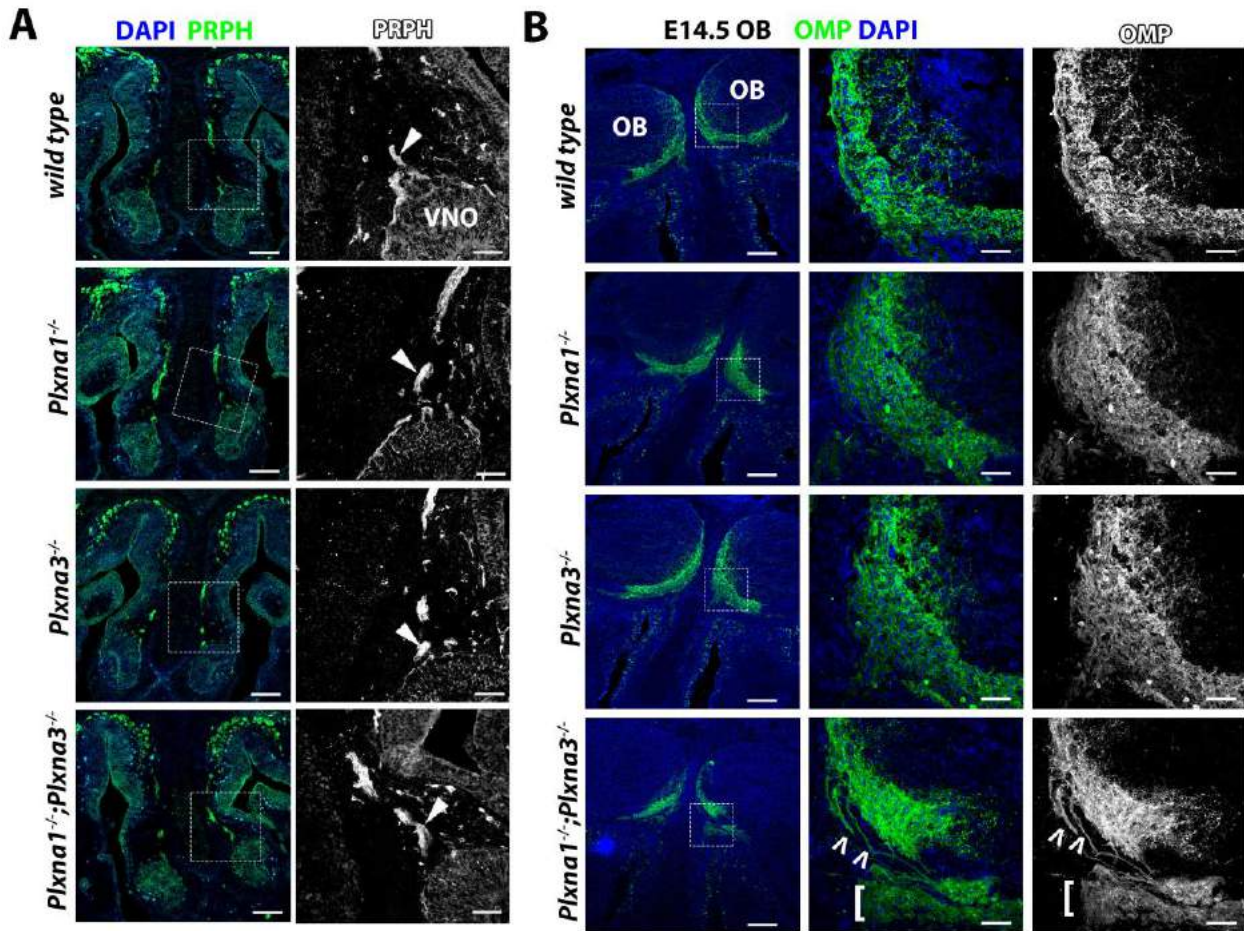


Fig. S6. Combined PLXNA1 and PLXNA3 loss does not preclude axon projection out of the VNO, but compromises olfactory axon projection.

(A) Coronal sections of E14.5 mouse heads of the indicated genotypes at the level of VNO were immunolabelled for PRPH to reveal VN and cVN axons and counterstained with DAPI. White boxes indicate areas shown at higher magnification on the right of the corresponding panel as the single channel for PRPH in grey scale. Solid arrowheads indicate PPRH⁺ axons that emerge from the VNO and therefore represent intermingled VN and cVN axons. Scale bars: 125 and 40 μm for lower and higher magnifications, respectively.

(B) Coronal sections of E14.5 mouse heads of the indicated genotypes were immunolabelled for OMP to reveal OLF axons and were counterstained with DAPI. White boxes indicate areas shown at higher magnification adjacent to the corresponding image, including single channels for OMP in grey scale. Open arrowheads indicate examples of defasciculated axons, whereas the brackets indicate an area with abnormal OMP⁺ axons below the ventro-medial OB.

Scale bars: 150 and 50 μm (higher and lower magnifications, respectively).

Abbreviations: VNO, vomeronasal organ; OB, olfactory bulb.

Table S1.

GnRH+ cell number in E14.5 mouse heads of the indicated genotypes. CP, cribriform plate. Data are shown as mean \pm s.d. and P-values were calculated with a one-way ANOVA followed by a Dunnett's test for mutants relative to wild type; ***P < 0.001; **P < 0.01; *P < 0.05; ns, not significant (P > 0.05).

Genotype	Nose	CP	Forebrain	Total
Wild type (n = 4 mice)	261.5 \pm 59.04	263.5 \pm 16.18	591.8 \pm 104.0	1228 \pm 154.9
Plxna1^{-/-} (n = 6 mice)	266.3 \pm 71.16 ns	377.0 \pm 96.71 ns	521.0 \pm 131.3 ns	1164 \pm 136.6 ns
Plxna3^{-/-} (n = 3 mice)	372.0 \pm 71.63 ns	381.7 \pm 81.38 ns	520.3 \pm 112.5 ns	1274 \pm 133.1 ns
Plxna1^{-/-};Plxna3^{-/-} (n = 4 mice)	429.5 \pm 118.5 *	519.5 \pm 101.6 **	183.5 \pm 50.13 ***	1133 \pm 188.2 ns

Table S2.

Mendelian ratio of postnatal mice in 5 different litters obtained from matings of *Plxna1^{+/-};Plxna3^{+/-}* females with *Plxna1^{+/-};Plxna3^{y/-}* males.

Genotype	Number of mice in litters	% expected			% observed		
		total	male	female	total	male	female
<i>Plxna1^{+/+};Plxna3^{y/+}, Plxna1^{+/+};Plxna3^{+/-}</i>	6	12.50	6.25	6.25	10.79	8.97	1.82
<i>Plxna1^{+/-};Plxna3^{y/+}</i>	8	12.50	12.50	0	14.58	14.27	0
<i>Plxna1^{-/-};Plxna3^{y/+}, Plxna1^{-/-};Plxna3^{+/-}</i>	8	12.50	6.25	6.25	14.75	9.45	5.30
<i>Plxna1^{+/+};Plxna3^{y/-}, Plxna1^{+/+};Plxna3^{-/-}</i>	9	12.50	6.25	6.25	16.09	16.09	0
<i>Plxna1^{+/-};Plxna3^{+/-}</i>	4	12.50	0	12.5	6.97	0	6.97
<i>Plxna1^{+/-};Plxna3^{y/-}, Plxna1^{+/-};Plxna3^{-/-}</i>	15	25.00	12.50	12.5	27.33	6.67	18.33
<i>Plxna1^{-/-};Plxna3^{y/-}, Plxna1^{-/-};Plxna3^{-/-}</i>	5	12.50	6.25	6.25	9.48	10.00	2.50

Table S3.

Total GnRH neuron number in postnatal MPOAs from mice of the indicated genotypes; data are shown as mean \pm s.d.; P-values were calculated with a one-way ANOVA followed by a Dunnett's test for mutants relative to wild type; *P < 0.05, ***P < 0.001, ****P < 0.0001; ns, not significant (P > 0.05).

Genotype	MPOA GnRH neuron number
Wild type (n = 5 males)	691.0 \pm 153.4
Plxna1^{-/-} (n = 5 males)	466.4 \pm 93.0 (*)
Plxna3^{y/-} (n = 4 males)	637.0 \pm 88.04 (ns)
Plxna1^{-/-};Plxna3^{-/-}(y) (n = 4; 3 males, 1 female)	143.3 \pm 41.91 (****)
Plxna1^{-/-};Plxna3^{+/-} (n = 2 females)	231 \pm 79.2 (***)

Table S4.

Hemisphere and OB area in images of brains dissected from P60 mice of the indicated genotypes, indicated as mean \pm s.d.; P-values were calculated with a one-way ANOVA followed by a Dunnett's test for mutants relative to wild type; ns, not significant (P > 0.05).

Genotype	Hemisphere area (mm ²)	OB area (mm ²)
Wild type (n = 3 mice; 2 males, 1 female)	222.0 \pm 6.21	26.53 \pm 4.12
Plxna1^{-/-} (n = 2 males)	225.8 \pm 14.89 (ns)	33.15 \pm 1.29 (ns)
Plxna3^{y/-} (n = 3 males)	224.1 \pm 10.26 (ns)	28.98 \pm 1.75 (ns)
Plxna1^{-/-};Plxna3^{-/-}(y) (n = 3; 2 males, 1 female)	215.4 \pm 8.09 (ns)	29.31 \pm 2.06 (ns)